Carcinogenesis vol.33 no.5 pp.1031–1039, 2012
doi:10.1093/carcin/bgs128
Advance Access publication March 20, 2012

The oncoprotein ErbB3 is endocytosed in the absence of added ligand in a clathrin-dependent manner

Malgorzata Magdalena Sak[1,2,†], Kamilla Breen[1,3,†], Sissel Beate Rønning[1,4], Nina Marie Pedersen[1,5], Vibeke Bertelsen[1], Espen Stang[2] and Inger Helene Madshus[1,2,*]

[1]Institute of Clinical Medicine, University of Oslo, Rikshospitalet, 0027 Oslo, Norway and [2]Department of Pathology, Oslo University Hospital, Rikshospitalet, PO Box 4950, Nydalen, 0424 Oslo, Norway

[3]Present address: Institute of Basic Medical Sciences, University of Oslo, 0317 Oslo, Norway

[4]Present address: Nofima AS, Osloveien 1, 1430 Ås, Norway

[5]Present address: Centre for Cancer Biomedicine, University of Oslo, Oslo, Norway and Department of Biochemistry, the Norwegian Radium Hospital, Montebello, 0310 Oslo, Norway

[*]To whom correspondence should be addressed. Tel: +47 23073536; Fax: +47 23071511;
Email: i.h.madshus@medisin.uio.no

The oncoprotein ErbB3 is overexpressed in several human cancers, for example in pancreatic adenocarcinoma and in ovarian cancers, and ErbB3-containing heterodimers have been demonstrated to be potent signaling units in carcinogenesis. This especially applies to ErbB2–ErbB3 and epidermal growth factor receptor (EGFR)–ErbB3 heterodimers providing anti-apoptotic signaling. Relatively little is understood about the signaling of EGFR–ErbB3 heterodimers and especially about mechanisms involved in downregulation of ErbB3 from the plasma membrane. This is in contrast to EGFR homodimers, for which trafficking has been extensively characterized. In the present study, we have investigated mechanisms involved in endocytosis of ErbB3 in porcine aortic endothelial cells stably expressing either ErbB3 only or stably expressing ErbB3 and EGFR. Our data show that ErbB3 is endocytosed in the absence of added ligand, independently of its tyrosine phosphorylation state and in a clathrin-dependent manner. Functional EGFR–ErbB3 heterodimers were observed to be formed, and dimerization with ErbB3 was observed to negatively affect endocytosis of the EGFR.

Introduction

The ErbB family of receptor tyrosine kinases induce growth, differentiation and survival signaling in a variety of cell types by conveying signals upon binding of different ligands [reviewed in refs. 1–3]. The ErbB family consists of four closely related members: epidermal growth factor (EGF) receptor (EGFR, also known as ErbB1 or HER1), ErbB2 (HER2/Neu), ErbB3 (HER3) and ErbB4 (HER4). Signal transduction by these receptor tyrosine kinases depends on their dimerization (4,5). Despite their overall similar structure, ErbB proteins differ in their properties with respect to ligand-binding and kinase activity. EGFR and ErbB4 both bind ligands and form homo- and/or heterodimers, whereas ErbB2 is an orphan receptor incapable of binding ligand (6,7). While non-liganded receptors normally exist in a folded conformation preventing dimerization, ErbB2 has a constitutively extended conformation, making it constantly available for interaction with other ErbB proteins (8). ErbB3 can bind several ligands but was for a long time considered kinase dead (9–11). It was recently reported that ErbB3 in fact possesses weak tyrosine kinase activity but that efficient phosphorylation depends on heterodimerization (12,13). ErbB3 is also considered unable to form homodimers (14). The ErbB2–ErbB3 signaling complex is potent in mediating anti-apoptotic signaling (15), and recent studies have reported a critical role for ErbB3 in mediating EGFR-dependent proliferative signaling in pancreatic cancers (16). Even though ErbB3 has little oncogenic potential in its own capacity, when *trans*-phosphorylated, it efficiently induces activation of phosphoinositide 3-kinase, since it has six binding sites for the p85 subunit (17–19). These characteristics make ErbB3 an important player in tumor biology and an interesting target for anticancer therapy [reviewed in refs. 8,20–22].

Receptor downregulation is essential to fine-tune signaling [reviewed in ref. 23]. While EGFR is known to undergo EGF-induced endocytosis and lysosomal degradation [reviewed in refs. 8,24,25], several lines of evidence have suggested that other ErbB proteins are endocytosed inefficiently (26–28). ErbB2, -3 and -4 have, in contrast to EGFR, been reported not to interact with the clathrin adaptor protein complex-2 and therefore to be inefficiently internalized (26). The full explanation for ErbB2's endocytosis impairment is still unclear but could result from stabilization upon interaction of ErbB2 with heat shock protein Hsp90 (29). Furthermore, it appears that unlike EGFR homodimers, ligand-activated EGFR–ErbB2 heterodimers are unable to induce formation of clathrin-coated pits and/or to translocate into clathrin-coated pits (28,30). To what extent ErbB3 is endocytosed and whether heterodimerization and transactivation are required for internalization of ErbB3 has also been unclear. ErbB3 was first suggested to be endocytosis impaired, based on a study demonstrating that the chimeric receptor consisting of the EGFR extracellular domain and the ErbB3 intracellular domain failed to efficiently internalize ^{125}I-EGF (26). It was later reported that ErbB3 had a very low rate of ligand-dependent internalization (31), whereas it was in other studies proposed that ErbB3 was internalized and efficiently recycled (27). It has also by several authors been reported that ErbB3 has a relatively short half-life (around 2.5–3.5 h) (27,32,33). The ErbB3 ligand heregulin (HRG) exists in a number of isoforms, which all share an EGF-like domain but differ with respect to the N-terminal domain (32). A short recombinant HRG-β1, containing the EGF-like domain only (herein referred to as HRG-β1), was demonstrated to have no effect on the turnover of surface-localized ErbB3. However, downregulation of ErbB3 was enhanced in MCF-7 breast cancer cells by incubation with a recombinant HRG-β1, containing the immunoglobulin (Ig)-like domain, herein referred to as HRG-β1 extracellular domain (HRG-β1 ECD). This could be due to increased ability of HRG-β1 ECD to disrupt higher order oligomers of ErbB3 (32). The ubiquitin ligase neuregulin receptor degradation protein-1 (Nrdp1) has further been reported to be involved in the constitutive ubiquitination and proteasomal degradation of ErbB3 (34,35). Increased stability of Nrdp1 has in turn been suggested to correlate with increased levels of the deubiquitinating protein Ubiquitin C-terminal hydrolase 8 (USP8, also called UBPY) (36). Interestingly, USP8 appears to be upregulated by binding of HRG-β1 to ErbB3. The half-life of ErbB3 was reported to be 2.5 h in the absence of HRG-β1 but 0.5 h in the presence of HRG-β1 (33). It should be noted that some cancer cells, in addition to having increased levels of ErbB proteins, have decreased levels of Nrdp1, thereby making the ubiquitin-dependent control of ErbB3 levels inefficient (37).

Endocytosis of signaling receptors is important in counteraction of carcinogenesis. This is because upon internalization, the receptor cannot longer bind growth factors localized extracellularly. Furthermore, proteins in early endosomes will either be recycled to the

Abbreviations: CHC, clathrin heavy chain; CHX, cycloheximide; EEA1, early endosome antigen 1; EGF, epidermal growth factor; EGFR, epidermal growth factor receptor; HRG, heregulin; MEM, minimal essential medium; Nrdp1, neuregulin receptor degradation protein-1; PAE, porcine aortic endothelial; siRNA, small interfering RNA.

[†]These authors contributed equally to this work.

plasma membrane or sorted to late endosomes/lysosomes, where degradation of both ErbB proteins and their bound ligands will occur. The extent of ErbB3 endocytosis and the potential mechanisms involved in ErbB3 internalization are still unclear and debated. We have in the current study investigated characteristics of ErbB3 endocytosis. We now report that like in case of ErbB2, dimerization of ErbB3 with EGFR has an inhibitory effect on endocytosis of EGF. However, the inhibitory effect on EGFR downregulation is less pronounced than in case of EGFR–ErbB2 dimers. We also demonstrate that ErbB3 is endocytosed in the absence of added ligand in a clathrin-dependent manner but independently of its tyrosine phosphorylation.

Materials and methods

Materials

Human recombinant EGF was from Bachem AG (Bubendorf, Switzerland), HRG-β1 ECD was from R&D Systems (Minneapolis, MN) and TO-PRO-3 iodide was from Life Technologies (Carlsbad, CA). Other chemicals were from Sigma Chemicals Co. (St Louis, MO) unless otherwise noted.

Cell culture and treatment

HeLa cells, MCF-7 cells and SK-BR-3 cells were grown in Dulbecco's modified Eagle's medium with L-glutamine (2 mM). Porcine aortic endothelial (PAE) cell lines were grown in Ham's F-12 medium with L-glutamine (2 mM). Media were from the Lonza Group Ltd (Basel, Switzerland). For all cells, 0.5 × penicillin–streptomycin (Lonza Group Ltd) and 10% fetal bovine serum were routinely used, whereas for SK-BR-3 cells, 15% fetal bovine serum was used. Stably transfected PAE cells expressing EGFR only (PAE.B2, here referred to as PAE.EGFR) were from Alexander Sorkin (University of Pittsburgh, Pittsburgh, PA). PAE.EGFR.ErbB2 and PAE.EGFR.ErbB3 cells were described previously (28,38). PAE.ErbB3 cells were established by stable transfection of PAE cells (obtained from Carl-Henrik Heldin, Ludwig Institute for Cancer Research, Uppsala, Sweden), using the plasmid pcDNA3.1 Hygro(+) ErbB3 (38) and standard single cell cloning procedures (39). The transfection reagent FuGENE 6 (Roche Diagnostics, Indianapolis, IN) was used in accordance with the manufacturer's recommendations. Geniticin (G418) (400 μg/ml), zeocin (30 μg/ml) and hygromycin (60 μg/ml) (all from Life Technologies) were added to the media used for the stably transfected PAE cells to select for clones stably expressing EGFR, ErbB2 and ErbB3, respectively. For receptor expression levels in HeLa, SK-BR-3 and PAE cells, see Supplementary Figure S1, available at *Carcinogenesis* Online. For receptor activation experiments, 10 nM EGF (60 ng/ml), 10 nM HRG-β1 (80 ng/ml) or 10 nM HRG-β1 ECD (269 ng/ml) was added to cells in minimal essential medium (MEM) without bicarbonate (Life Technologies) in the presence of 0.1% bovine serum albumin. In experiments investigating downregulation from the plasma membrane and degradation of EGFR or ErbB3, 25 μg/ml cycloheximide (CHX) and 10 nM EGF, HRG-β1 or HRG-β1 ECD was added. For activation of c-Met, 1.25 nM hepatocyte growth factor (100 ng/ml) was used and to inhibit the c-Met kinase activity, cells were preincubated with 2 μM SU11274 overnight and then serum starved in MEM with 2 μM SU11274 for 15 min before incubation with hepatocyte growth factor in the presence of SU11274. For inhibition of ErbB3 phosphorylation, 5 μM AG1478 (Life Technologies) was used, including 2 h serum starvation and preincubation with MEM containing AG1478.

Plasmids and small interfering RNAs

For knockdown of clathrin heavy chain (CHC), the target sequence was GCAAUGAGCUGUUUGAAGA (40). Control cells were transfected with either Silencer Negative Control #1 or with small interfering RNA (siRNA) to green fluorescent protein (target sequence: GCACAAGCUCCACUGCAACUACA), as indicated in figure legends and as described previously (41). All siRNA duplexes were synthesized and annealed by Life Technologies. For transient expression of ErbB3, the pcDNA3.1 Hygro(+) ErbB3 plasmid was used (38).

Transfection of cells

Cells were transfected with siRNA twice with a 48 h interval using Lipofectamine™ 2000 (Life Technologies) according to the manufacturer's recommendations, using 28 μl Lipofectamine™ 2000 and 750 pmol siRNA for each T-75 tissue culture flask. Transient transfection with the ErbB3-encoding plasmid was performed with FuGENE 6 transfection reagent 20–24 h prior to experiments, according to the manufacturer's recommendations.

Antibodies

Mouse anti-ErbB3 and mouse anti-EGFR antibodies were from Lab Vision (Fremont, CA). Sheep anti-EGFR antibody was from Fitzgerald Industries International (Concord, MA). Rabbit anti-ErbB3, goat anti-Akt, rabbit anti-Erk and rabbit anti-Numb antibodies were from Santa Cruz Biotechnology (Santa Cruz, CA). Rabbit anti-β-actin and rabbit anti-β-tubulin antibodies were from Abcam (Cambridge, UK). Rabbit anti-p-ErbB3 (pY1289), rabbit anti-p-Erk and rabbit anti-p-Akt antibodies were from Cell Signaling Technology (Danvers, MA). Mouse anti-p-EGFR (pY1173) and rabbit anti-early endosome antigen 1 (EEA1) antibodies were from Millipore (Billerica, MA). Alexa Fluor 488-conjugated goat anti-mouse IgG, Alexa Fluor 647-conjugated donkey anti-rabbit IgG, rabbit anti-p-Met (pY1234/1235) and mouse anti-transferrin receptor antibodies were from Life Technologies. Rhodamine-Red-X-conjugated donkey anti-rabbit IgG, phycoerythrin-conjugated goat anti-mouse IgG and peroxidase-conjugated donkey anti-rabbit, anti-sheep, anti-goat and anti-mouse IgG antibodies were from Jackson ImmunoResearch Laboratories (West Grove, PA). Mouse anti-CHC antibody was from BD Biosciences (Erembodegem, Belgium).

Western blotting

Cell lysates were subjected to sodium dodecyl sulfate–polyacrylamide gel electrophoresis and western blotting as described (42), and proteins were detected using SuperSignal West Dura Extended Duration Substrate from Pierce (Thermo Fisher Scientific, Rockford, IL). Proteins were visualized using the KODAK Image Station 4000R from Carestream Health (Rochester, NY). Quantifications were performed using KODAK Molecular Imaging software, version 4.0.

Internalization of ^{125}I-EGF

Internalization of ^{125}I-EGF (PerkinElmer, Waltham, MA) was performed essentially as described (41). Cells were incubated with ^{125}I-EGF (1 ng/ml) alone or with ^{125}I-EGF in combination with 10 nM HRG-β1 or HRG-β1 ECD for the times indicated. Cells were lysed in 1% sodium dodecyl sulfate in phosphate-buffered saline for 10 min on ice, and the radioactivity in the fractions containing cell surface-bound and internalized ^{125}I-EGF was measured in a γ-counter (1470 Wallac WIZARD, PerkinElmer). Statistical significance was tested using the two-tailed Student's *t*-test.

Flow cytometry analysis

Cells were incubated as described in figure legends before being trypsinized and fixed in 4% paraformaldehyde (Riedel-de Haën, Seelze, Germany) in Sorensen's phosphate buffer. Flow cytometry analysis was performed as described previously (43), using mouse anti-ErbB3, mouse anti-EGFR and phycoerythrin-conjugated goat anti-mouse IgG antibodies. The samples were analyzed using a FACS Calibur flow cytometer (BD Biosciences, San Jose, CA). A minimum of 10 000 cells were analyzed for each sample. Unstained cells, incubated with the secondary antibody only, were included in the analysis to show background fluorescence. Statistical significance was tested using the two-tailed Student's *t*-test.

Immunocytochemistry and confocal microscopy

Cells were grown in 6 cm culture dishes and incubated as described in figure legends before being fixed in 4% paraformaldehyde and immunostained as described (28). The cells were examined by confocal microscopy analysis (Leica TCS SP; Leica Microsystems AG, Wetzlar, Germany and Olympus FluoView FV1000; Olympus Corporation, Tokyo, Japan), and pictures were processed using Adobe Photoshop CS4.

Results

ErbB3 was endocytosed in the absence of added ligand, independently of other ErbB proteins and independently of its phosphorylation

Since downregulation of ErbB3 from the plasma membrane is poorly understood, we investigated the efficiency by which ErbB3 was downregulated in PAE.EGFR.ErbB3 cells. In non-stimulated cells immunolabeled with antibodies to ErbB3 or EGFR, ErbB3 was found both at the plasma membrane and in intracellular vesicles (Figure 1A, upper panels). These vesicles were both EEA1 positive and EEA1 negative. In contrast, non-liganded EGFR appeared mostly at the cell surface, not colocalizing with EEA1 (Figure 1A, lower panels).

To confirm that ErbB3 was internalized from the plasma membrane, PAE.EGFR.ErbB3 cells were incubated on ice with an antibody that recognized the extracellular part of ErbB3 (44). The cells were then washed to remove unbound antibody and either left on ice or chased at 37°C for 15 min before fixation. While cells incubated on ice displayed clear plasma membrane staining for the

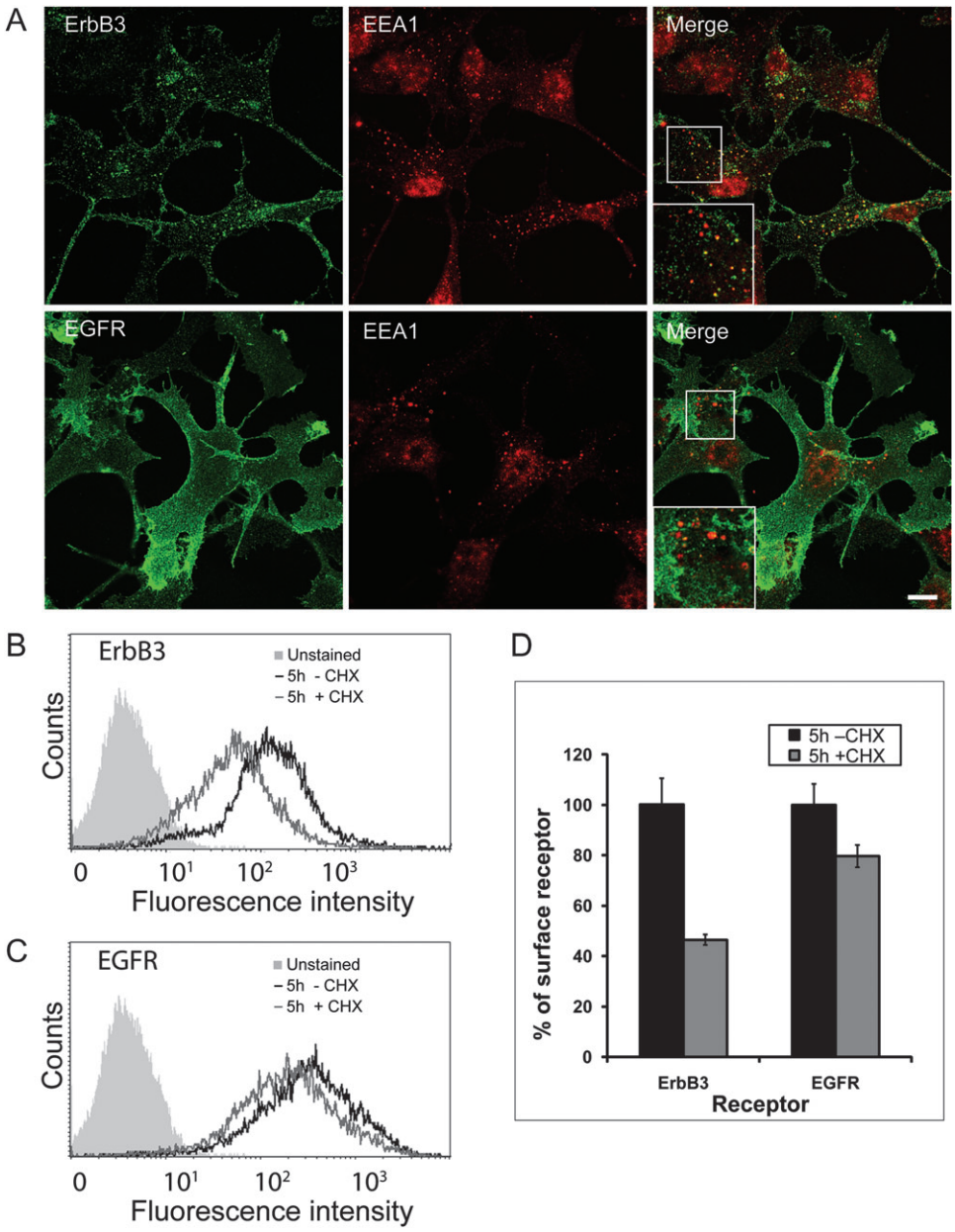

Fig. 1. ErbB3 was localized to endosomes and downregulated from the plasma membrane in the absence of added ligand. (**A**) PAE.EGFR.ErbB3 cells were fixed, permeabilized and immunostained with mouse anti-ErbB3 antibody (upper left panel) or mouse anti-EGFR antibody (lower left panel) and rabbit anti-EEA1 antibody (middle panels), followed by Alexa Fluor 488-conjugated anti-mouse and Alexa Fluor 647-conjugated anti-rabbit antibodies. The cells were subsequently analyzed by confocal microscopy. Right panels represent merged left and middle panels. Scale bar, 10 μm. The framed areas are shown at higher magnification in the lower left corner of the respective micrographs. (**B**–**D**) PAE.EGFR.ErbB3 cells were incubated with or without CHX (25 μg/ml) for 5 h at 37°C, then trypsinized, fixed and labeled with mouse anti-ErbB3 (B) or mouse anti-EGFR antibodies (C) followed by phycoerythrin-conjugated anti-mouse antibodies. The surface level of ErbB3 and EGFR was analyzed by flow cytometry. The curves represent unstained cells (only secondary antibody) and one of three parallels for each condition from a representative experiment. (D) The average median values of four experiments with three parallels each, ±pooled standard deviation, were plotted. The data are presented as percentage of control values from cells incubated without CHX.

anti-ErbB3 antibody (Supplementary Figure S2A, available at *Carcinogenesis* Online), in cells incubated at 37°C, anti-ErbB3 antibody was also observed in EEA1 positive endosomes (Supplementary Figure S2B and D, available at *Carcinogenesis* Online). To make sure that endocytosis of ErbB3 was not induced by the antibody, the cells were incubated with or without anti-ErbB3 antibody for 30 min on ice and subsequently washed and chased in MEM for 30 min at 37°C. Upon fixation, the cells were stained with the same antibody before the amount of anti-ErbB3 antibody at the plasma membrane was analyzed by flow cytometry. The cells that had been preincubated with antibody showed no reduction in ErbB3 plasma membrane level (Supplementary Figure S2E and F, available at *Carcinogenesis* Online). Instead, the level of ErbB3 at the plasma membrane was slightly increased. This increase could potentially be explained by longer incubation with the antibody allowing increased binding (prefixation and postfixation incubation) and/or by increased antibody affinity for native (prefixation) ErbB3 compared with ErbB3 exposed to fixatives.

To directly compare the rate of downregulation of EGFR and ErbB3 from the plasma membrane, PAE.EGFR.ErbB3 cells were incubated with or without CHX for 5 h at 37°C, and the surface levels of EGFR and ErbB3 were then analyzed by flow cytometry. The rate

of ErbB3 downregulation from the cell surface (Figure 1B) was significantly higher than for the EGFR (Figure 1C). While >50% of ErbB3 was downregulated from the plasma membrane upon 5 h incubation, the level of EGFR was only reduced by 20% (Figure 1D).

We additionally examined endocytosis of ErbB3 in human cells. Since endogenous ErbB3 was not detectable in HeLa cells (Supplementary Figure S1A, available at *Carcinogenesis* Online), we transiently transfected HeLa cells with an ErbB3-encoding plasmid. Upon incubation with anti-ErbB3 antibody and chase for 30 min at 37°C, anti-ErbB3 antibodies localized intracellularly in both SK-BR-3 cells (Supplementary Figure S3, available at *Carcinogenesis* Online, upper panels), HeLa cells (Supplementary Figure S3, available at *Carcinogenesis* Online, lower panels) and MCF-7 cells (Supplementary Figure S4B, available at *Carcinogenesis* Online). A large fraction of the anti-ErbB3 positive vesicles was found to colocalize with EEA1 (Supplementary Figure S3, available at *Carcinogenesis* Online). ErbB3 was also internalized in PAE.ErbB3 cells with no expression of other ErbB proteins (Figures 2A and 3B).

ErbB3 has been found to dimerize with and be activated by c-Met (45–47), and PAE cells endogenously express c-Met (48). In order to investigate the potential role of cross talk between c-Met and ErbB3 during internalization, PAE.ErbB3 cells were incubated with the c-Met kinase inhibitor SU11274 (49). As demonstrated in Figure 2A, ErbB3 was internalized and colocalized with EEA1 also in cells incubated with the c-Met inhibitor, even though western blot analysis of cells incubated with SU11274 demonstrated efficient inhibition of c-Met phosphorylation upon incubation with hepatocyte growth factor (Figure 2B).

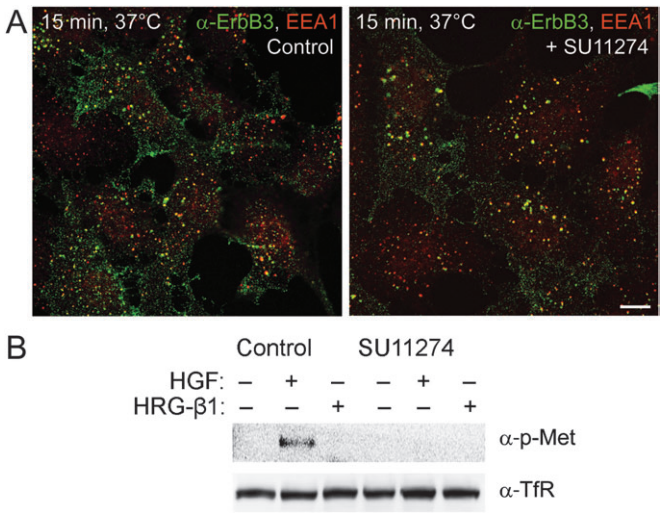

Fig. 2. ErbB3 was endocytosed in the absence of other ErbB proteins and independently of the c-Met kinase activity. (**A**) PAE.ErbB3 cells were preincubated overnight with the c-Met kinase inhibitor SU11274 (2 μM) in dimethyl sulfoxide (DMSO) or with DMSO alone (control). The cells were then incubated with mouse anti-ErbB3 (in MEM with 0.1% bovine serum albumin ±kinase inhibitor) for 30 min on ice before washing in ice-cold phosphate-buffered saline and chasing in MEM (±kinase inhibitor) for 15 min at 37°C before fixation. After permeabilization, subcellular localization of the anti-ErbB3 antibody was detected with Alexa Fluor 488-conjugated anti-mouse antibody. Early endosomes were localized with rabbit anti-EEA1 antibody followed by Alexa Fluor 647-conjugated anti-rabbit antibody. The cells were analyzed by confocal microscopy. Scale bar, 10 μm. (**B**) PAE.ErbB3 cells were preincubated overnight with SU11274 (2 μM) in DMSO or with DMSO alone (Control). The cells were then incubated (±kinase inhibitor) without ligand (−), with 1.25 nM hepatocyte growth factor (HGF) or 10 nM HRG-β1 for 5 min at 37°C. The cells were lysed and subjected to western blotting. Phosphorylated c-Met was detected with rabbit anti-p-Met (pY1234/1235) antibody. Antibody to the transferrin receptor (α-TfR) was used as loading control. The figure shows one representative experiment of three.

We observed a small constitutive phosphorylation of ErbB3 in PAE.ErbB3 cells, accompanied by constitutive activation of Erk and Akt (Figure 3A). As also demonstrated in Figure 3A, phosphorylation of ErbB3, Erk and Akt increased upon incubation with HRG-β1. The constitutive, as well as the HRG-β1-induced signaling, was not affected by c-Met kinase inhibition (data not shown). It has been proposed that c-Src can phosphorylate ErbB3 and that this phosphorylation can be reduced using an inhibitor of c-Src kinase activity (50,51). However, when we used the c-Src kinase specific inhibitor SU6656 (52), we did not observe any effect on the ErbB3 phosphorylation (data not shown). The EGFR kinase inhibitor, AG1478, has been reported to inhibit HRG-β1-induced phosphorylation of ErbB2 and ErbB3, in addition to inhibiting the EGFR (53). Consistently, when we incubated PAE.ErbB3 cells with AG1478, both the constitutive and the HRG-β1-induced phosphorylation of ErbB3, Erk and Akt were efficiently blocked (Figure 3A). This could either suggest that ErbB3 to some extent forms homodimers and that AG1478 is not fully EGFR specific or that there are small amounts of AG1478-inhibitable non-defined kinase activity in PAE cells. Internalization of ErbB3 was, however, not inhibited upon incubation with AG1478 (Figure 3B). Also in MCF-7 cells, did AG1478 efficiently block HRG-β1-induced signaling (Supplementary Figure S4A, available at *Carcinogenesis* Online) without having effect on ErbB3 internalization (Supplementary Figure S4B, available at *Carcinogenesis* Online). These data support the notion that ErbB3 is internalized in the absence

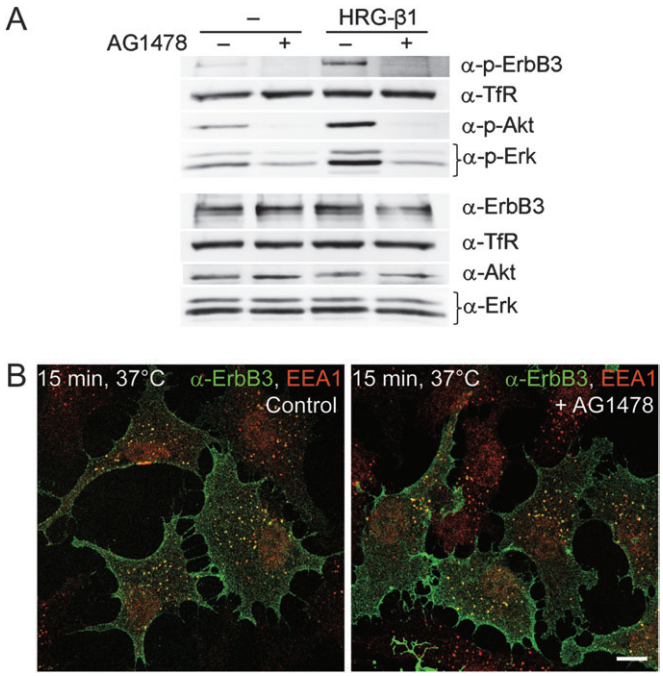

Fig. 3. ErbB3 was endocytosed independently of its phosphorylation. (**A**) PAE.ErbB3 cells were preincubated with or without the EGFR kinase inhibitor AG1478 (5 μM) for 2 h. The cells were then incubated (±kinase inhibitor) with or without 10 nM HRG-β1 for 3 min at 37°C. The cells were lysed and subjected to western blotting using antibodies to phosphorylated and total ErbB3, Akt and Erk. Antibody to transferrin receptor (α-TfR) was used as loading control. (**B**) PAE.ErbB3 cells were preincubated with or without AG1478 (5 μM) for 2 h. The cells were then incubated with mouse anti-ErbB3 antibody (in MEM with 0.1% bovine serum albumin ±kinase inhibitor) for 30 min on ice before washing in ice-cold phosphate-buffered saline and chasing in MEM (±kinase inhibitor) for 15 min at 37°C before fixation. After permeabilization, localization of anti-ErbB3 antibody was detected with Alexa Fluor 488-conjugated anti-mouse antibody. Early endosomes were localized with rabbit anti-EEA1 antibody followed by Alexa Fluor 647-conjugated anti-rabbit antibody. The cells were analyzed by confocal microscopy. Scale bar, 10 μm. The figure shows one representative experiment of three.

of added ligand and that endocytosis does not depend on ErbB3 phosphorylation.

Endocytosis of ErbB3 was clathrin dependent

To study by which endocytic pathway ErbB3 is internalized, we transfected PAE.EGFR.ErbB3 cells with siRNA to CHC. As demonstrated, the level of CHC was strongly reduced, whereas the level of ErbB3 remained almost unchanged (Figure 4A). Since EGFR is mainly endocytosed in a clathrin-dependent manner (40,54,55), EGF-induced downregulation of EGFR from the plasma membrane was used as a positive control. As expected, the EGFR level was also unchanged, and ligand-induced downregulation of EGFR was strongly inhibited in clathrin-depleted cells (Supplementary Figure S5A–C, available at *Carcinogenesis* Online). We then investigated the internalization of anti-ErbB3 antibodies and found that while cells transfected with control siRNA exhibited vesicular anti-ErbB3 staining (Figure 4B, left panel), cells depleted of clathrin displayed a strong plasma membrane staining (Figure 4B, right panel). The inhibition of ErbB3 endocytosis in cells transfected with siRNA to CHC was quantified manually. Data showed that depletion of CHC efficiently inhibited endocytosis of ErbB3, since $<10\%$ of the cells showed endosomal labeling for anti-ErbB3 (Figure 4C). Also, flow cytometry analysis confirmed that downregulation of ErbB3 from the plasma membrane in cells where CHC had been depleted was significantly inhibited (Figure 4D and E). CHC knockdown strongly reduced ErbB3 internalization also in MCF-7 cells (Supplementary Figure S5D and E, available at *Carcinogenesis* Online). We thus conclude that the observed internalization of ErbB3 is clathrin dependent.

ErbB3 was activated upon incubation with ligand but was degraded independently of added ligand

To investigate whether ErbB3 and EGFR formed functional heterodimers in PAE cells, we investigated receptor phosphorylation in PAE.EGFR.ErbB3 cells. The cells were incubated with or without EGF, HRG-β1, HRG-β1 ECD or combinations of each HRG and EGF. Cell lysates were then subjected to western blotting using phosphotyrosine-specific antibodies. Although, when compared with PAE.ErbB3 cells, PAE.EGFR.ErbB3 cells express less ErbB3 (see Supplementary Figure S1, available at *Carcinogenesis* Online), HRG-β1- and HRG-β1 ECD-induced phosphorylation of ErbB3 were most pronounced in PAE.EGFR.ErbB3 cells (Figure 5A compare with Figure 3A). This strongly suggests that HRG can induce formation of EGFR–ErbB3 heterodimeres followed by EGFR-mediated *trans*-phosphorylation of ErbB3. Phosphorylation of ErbB3 was, however, not increased upon incubation with EGF. Activation of EGFR was clearly induced by addition of EGF but not by HRG-β1 or HRG-β1 ECD (Figure 5A). This is consistent with the notion that while ErbB3 can transactivate and be *trans*-phosphorylated by the EGFR, the EGFR cannot be *trans*-phosphorylated by ErbB3, which has marginal kinase activity (13). In the samples where EGF was added in

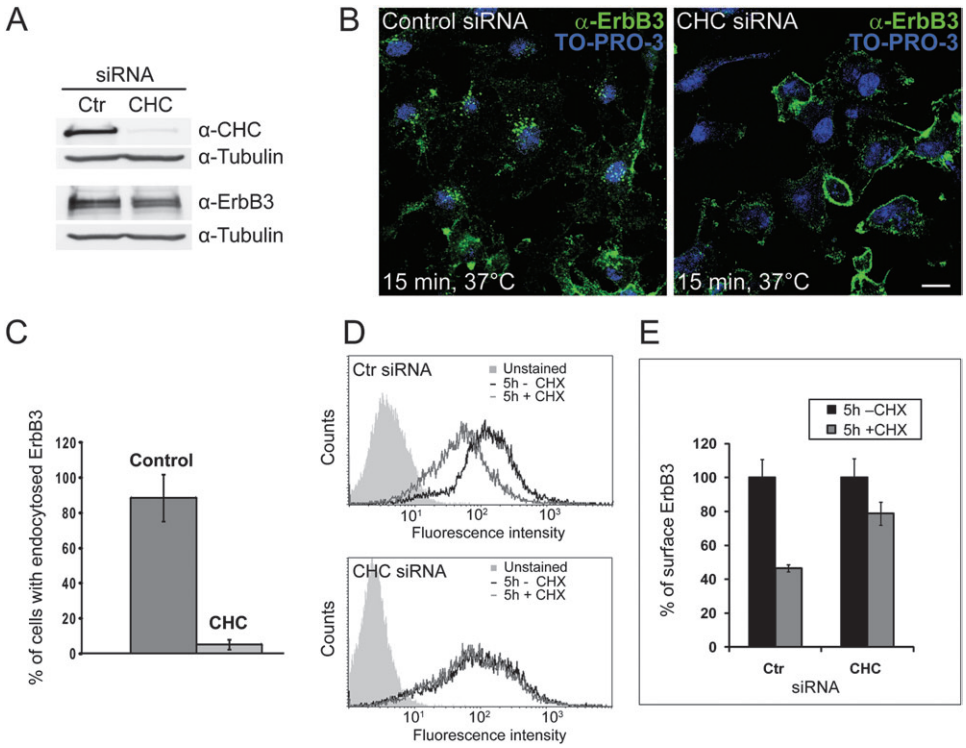

Fig. 4. Endocytosis of ErbB3 was inhibited upon clathrin knockdown. (**A**) PAE.EGFR.ErbB3 cells transfected with Silencer Negative Control siRNA or with siRNA against CHC were lysed and subjected to western blotting using mouse anti-CHC and rabbit anti-ErbB3 antibodies. Rabbit anti-tubulin antibody was used as loading control. (**B**) PAE.EGFR.ErbB3 cells transfected with either Silencer Negative Control siRNA (left panel) or siRNA to CHC (right panel). The cells were then incubated with mouse anti-ErbB3 antibody (in MEM with 0.1% bovine serum albumin) for 30 min on ice before washing in ice-cold phosphate-buffered saline and chasing in MEM for 15 min at 37°C before fixation. After permeabilization, localization of anti-ErbB3 antibody was detected with Alexa Fluor 488-conjugated anti-mouse antibody. Nuclei were stained with TO-PRO-3. The labeled cells were analyzed by confocal microscopy. Scale bar, 60 μm. (**C**) To quantify endocytosis in cells transfected with siRNA to CHC or with control siRNA (siRNA to green fluorescent protein), the cells were counted manually, classifying the cells with respect to content of vesicles containing anti-ErbB3 antibody. A minimum of 50 cells were counted from each of two separate experiments. The cells showing endocytosis are presented as percentage of the total number of counted cells. Error bars indicate standard deviation. (**D**) PAE.EGFR.ErbB3 cells, transfected with Silencer Negative Control (upper panel) or CHC (lower panel) siRNA, were incubated with or without CHX (25 μg/ml) for 5 h at 37°C. The cells were trypsinized, fixed and labeled with mouse anti-ErbB3 and phycoerythrin-conjugated anti-mouse antibodies. The cell surface level of ErbB3 was analyzed by flow cytometry. The curves represent unstained cells (only secondary antibody) and one of three parallels for each condition from a representative experiment. (**E**) The average median values of four flow cytometry experiments with three parallels in each, ±pooled standard deviation, were plotted. The data are presented as percentage of control values from cells incubated without CHX.

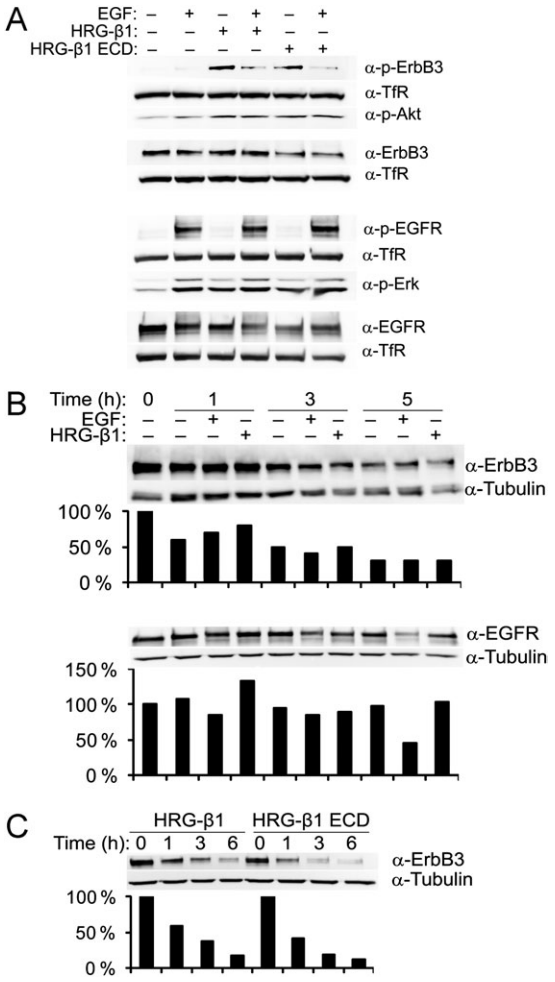

Fig. 5. ErbB3 was activated upon incubation with ligand but was degraded also in the absence of added ligand in PAE.EGFR.ErbB3 cells. (**A**) PAE.EGFR.ErbB3 cells were incubated with or without either 10 nM EGF, HRG-β1 or HRG-β1 ECD or both EGF and HRG-β1 or HRG-β1 ECD for 5 min at 37°C. The cells were then lysed and subjected to western blotting with antibodies to phosphorylated and total ErbB3 and phosphorylated Akt (upper panel) as well as phosphorylated and total EGFR and phosphorylated Erk (lower panel). Anti-transferrin receptor (TfR) antibody was used as loading control. The figure demonstrates one representative experiment of three. (**B**) PAE.EGFR.ErbB3 cells were incubated without ligand (−), with 10 nM EGF or HRG-β1 for 1, 3 or 5 h at 37°C. CHX (25 μg/ml) was included in all samples except for the control (0 h). The cells were lysed and subjected to western blotting using rabbit anti-ErbB3, sheep anti-EGFR and rabbit anti-Tubulin (loading control) antibodies. The figure shows one representative experiment of three. Net luminescence values of bands corresponding to ErbB3 or EGFR were normalized to the loading control, quantified and plotted as percentage of control (shown as histograms below the respective wells). (**C**) PAE.EGFR.ErbB3 cells were incubated with 10 nM HRG-β1 or HRG-β1 ECD for 1, 3 or 6 h at 37°C. CHX (25 μg/ml) was added to all samples except the control (0 h). Western blotting and quantification was performed as in (B). The figure demonstrates one representative experiment of three.

combination with either HRG-β1 or HRG-β1 ECD, there was a reduced phosphorylation of ErbB3 compared with upon incubation with each HRG variant alone. This could possibly be explained by EGF-induced formation of EGFR homodimers and consequently reduced amounts of EGFR available for ErbB3 interaction. The formation of functional dimers was confirmed by the observed activation of downstream targets (Figure 5A). Erk was activated upon incubation with either ligand but appeared most intensely phosphorylated in the presence of EGF. Akt phosphorylation, on the other hand, was strongest upon incubation with the HRGs, consistent with the finding that ErbB3 signals mainly through the phosphoinositide 3-kinase/Akt pathway (16).

HRG-β1 was previously demonstrated to have no effect on the turnover of surface-localized ErbB3, while downregulation of ErbB3 was enhanced by HRG-β1 ECD in MCF-7 breast cancer cells, and this could be due to better ability of HRG-β1 ECD to disrupt higher order oligomers of ErbB3 (32). To investigate whether the ligands had similar effect in PAE cells, we examined degradation of total ErbB3 in the presence of different ligands. PAE.EGFR.ErbB3 cells were incubated without ligand, with EGF, with HRG-β1 or with HRG-β1 ECD for different times in the presence of CHX. Then, the amount of residual ErbB3 and EGFR was studied by western blotting. While degradation of EGFR was clearly induced by EGF, ErbB3 was found to be efficiently degraded even in the absence of ligand (Figure 5B). Neither EGF nor HRG-β1 increased the ErbB3 degradation, arguing that ErbB3 is mostly degraded independently of added ligand. However, in consistence with the results of Warren *et al.* (32), our results demonstrated that degradation of ErbB3 was somewhat increased upon incubation with HRG-β1 ECD compared with upon incubation with HRG-β1 (Figure 5C).

HRG-β1 and HRG-β1 ECD both reduced EGF-induced endocytosis of the EGFR

We have previously demonstrated that overexpression of ErbB2 inhibited EGF-induced endocytosis of the EGFR (28). We therefore wanted to study whether overexpression of ErbB3 had a similar effect on endocytosis of the EGFR. The rate of ^{125}I-EGF internalization in PAE.EGFR cells, in PAE.EGFR.ErbB2 cells and in PAE.EGFR.ErbB3 cells was compared (Figure 6A). While the rate of endocytosis of ^{125}I-EGF was significantly inhibited in PAE.EGFR.ErbB2 cells, no significant inhibition was observed in PAE.EGFR.ErbB3 cells incubated with EGF only when compared with PAE.EGFR cells. To study the efficiency of EGFR downregulation from the cell surface, the same cell lines were incubated for 5 h in the presence of CHX, with or without EGF. The level of EGFR at the plasma membrane was investigated by flow cytometry analysis (Figure 6B). Consistent with data using ^{125}I-EGF, we found that downregulation of cell surface-localized EGFR was significantly inhibited in PAE.EGFR.ErbB2 cells but not in PAE.EGFR.ErbB3 cells. Altogether, our data thus argue that in contrast to ErbB2, expression of ErbB3 as such does not negatively impact on downregulation of the EGFR. However, when PAE.EGFR.ErbB3 cells were incubated with EGF in combination with either HRG-β1 or HRG-β1 ECD, the rate of EGF internalization was significantly reduced by ∼25% (Figure 6C). A similar result was observed in MCF-7 cells (Supplementary Figure S6A, available at *Carcinogenesis* Online). This is consistent with ligand-induced heterodimerization upon incubation with HRG-β1 and EGF, but not with EGF alone, and supports the idea that EGFR–ErbB3 heterodimers are internalized less efficiently than are EGFR homodimers. It should be noted that HRG-β1 ECD did not affect the internalization of EGF in cells not expressing ErbB3 (Supplementary Figure S6B, available at *Carcinogenesis* Online).

Discussion

We have previously demonstrated that ErbB2 negatively impacts on the ligand-induced downregulation of EGFR, presumably by tethering EGFR to the endocytosis-resistant ErbB2 (28,56). In the current study, we show that ErbB3, upon coexpression with EGFR in PAE cells, did not affect EGF-induced downregulation of EGFR from the plasma membrane. Although ErbB3 without bound ligand probably does not form heterodimers with the EGFR to same extent as does ErbB2, the data show that expression of ErbB3 as such does not have a negative impact on EGF-induced EGFR endocytosis. Ligands to ErbB3 have previously been shown to induce EGFR–ErbB3 heterodimerization (57–60). In line with this, we observed increased HRG-β1-induced phosphorylation of ErbB3 in PAE.EGFR.ErbB3 cells compared with in PAE.ErbB3 cells, supporting the formation of functional

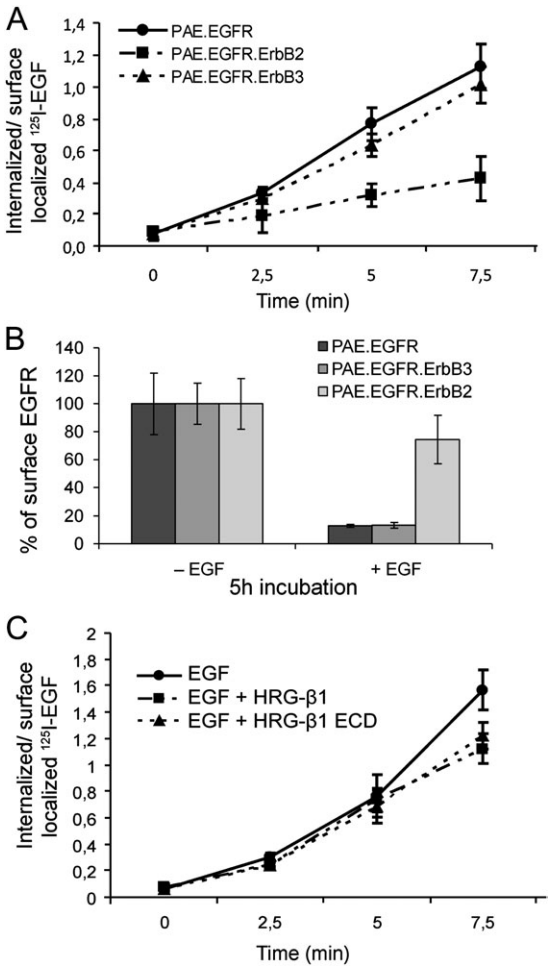

Fig. 6. Incubation with HRG-β1 and HRG-β1 ECD both reduced endocytosis of ^{125}I-EGF. (**A**) PAE.EGFR, PAE.EGFR.ErbB2 and PAE.EGFR.ErbB3 cells were incubated with ^{125}I-EGF (1 ng/ml) for 2.5, 5 and 7.5 min at 37°C, and the ratio of internalized to surface-localized ^{125}I-EGF was plotted as a function of time. The graph represents the average value of three independent experiments with four parallels each, ±pooled standard deviations. (**B**) The same cell lines as in (A) were incubated with CHX (25 μg/ml) and with or without 10 nM EGF for 5 h at 37°C. The cells were trypsinized, fixed and labeled with mouse anti-EGFR followed by phycoerythrin-conjugated anti-mouse antibodies. The cell surface level of EGFR was analyzed by flow cytometry. The average median values of three experiments with multiple parallels, ±pooled standard deviations, were plotted. The data are presented as percentage of control values from cells incubated without EGF. (**C**) PAE.EGFR.ErbB3 cells were incubated with ^{125}I-EGF (1 ng/ml) alone or with ^{125}I-EGF in combination with 10 nM HRG-β1 or HRG-β1 ECD for 2.5, 5 and 7.5 min at 37°C and the ratio of internalized/surface-localized ^{125}I-EGF was plotted as a function of time. The graph represents the average value of three independent experiments with four parallels each, ±pooled standard deviations.

EGFR–ErbB3 heterodimers. Also, when cells were incubated with EGF and HRG-β1 or HRG-β1 ECD, expression of ErbB3 did in fact reduce endocytosis of EGF, suggesting that ligand-induced EGFR–ErbB3 heterodimerization inhibits EGFR endocytosis. The results from the activation and internalization experiments may seem contradictory. We observed that incubation with HRG-β1 and EGF together caused reduced phosphorylation of ErbB3 when compared with incubation with HRG-β1 only and suggest that this is due to EGF-induced EGFR homodimerization and consequently reduced EGFR–ErbB3 heterodimerization. At the same time, we observed decreased internalization of EGF when HRG-β1 was added along with EGF and explained this with ligand-induced EGFR–ErbB3 heterodimerization. These two explanations are, however, not necessarily contradictory based on the following scenario. When HRG-β1 is added alone, EGFR–ErbB3 heterodimers will be formed and ErbB3 will be strongly *trans*-phosphorylated by the EGFR. When EGF is added alone, only EGFR homodimers will be formed, as shown by the lack of ErbB3 phosphorylation. This is in line with previous data showing EGF-induced phosphorylation of ErbB3 only in cells with high expression of ErbB3 (16), indicating inefficient EGF-induced EGFR–ErbB3 heterodimerization. When HRG-β1 and EGF are added together, the two ligands will, however, compete with respect to formation of different dimers. EGF will preferentially induce EGFR homodimers and reduce the amount of EGFR available for HRG-β1-induced heterodimerization. This will again decrease the level of ErbB3 phosphorylation. HRG-β1 will, on the other hand, still induce some EGFR–ErbB3 heterodimerization, and if EGFR–ErbB3 internalization is inhibited compared with EGFR–EGFR internalization, EGF bound to EGFR–ErbB3 heterodimers will be endocytosed less efficiently.

It has been demonstrated that ErbB3, in contrast to EGFR and ErbB2, displays a granular cytoplasmic distribution in various human tissues (61,62). In line with this, we observed that ErbB3, but not EGFR, localized to endosomes in the absence of added ligand. We also found that ErbB3 was internalized from the plasma membrane in the absence of added ligand and that internalized ErbB3 partly colocalized with EEA1 in PAE cells, HeLa cells and SK-BR-3 cells. Our data additionally demonstrated that downregulation of ErbB3 from the plasma membrane to a large extent depended on clathrin. It is, however, unclear by which mechanism ErbB3 is translocated into clathrin-coated pits and also which clathrin adaptor proteins can promote recruitment of ErbB3 to coated pits. It was reported that neither ErbB2, ErbB3 nor ErbB4 could associate with the α-adaptin subunit of the adaptor protein complex-2 (26,31). The E3 ubiquitin ligase Nrdp1 has been shown to interact with ErbB3 independently of HRG-β1 binding and to promote a steady state degradation of ErbB3 (33,35). One could therefore speculate that, like in case of the EGFR, ubiquitination serves as a signal for ErbB3 internalization. Flow cytometry experiments showed that while ∼55% of ErbB3 was lost from the cell surface within 5 h in control cells, ∼20% was lost also in clathrin-depleted cells. Although this downregulation could potentially be explained by inefficient knockdown of clathrin, it could also suggest alternative mechanisms of ErbB3 downregulation acting in parallel with the clathrin-dependent endocytic pathway.

As demonstrated in this study, endocytosis of ErbB3 can occur independently of other ErbB proteins as well as independently of c-Met kinase activity. We have also demonstrated that ErbB3 was efficiently degraded and that the degradation of ErbB3 was not significantly affected by EGF or HRG-β1. However, consistent with previously reported findings (32), the degradation of ErbB3 was slightly enhanced by HRG-β1 ECD. Our data argue that ErbB3 is internalized regardless of its state of phosphorylation. Although ErbB3 has an impaired kinase activity (9–11), ErbB3 was demonstrated to have sufficient kinase activity to *trans*-autophosphorylate its intracellular domain (13). Consistently, we observed HRG-β1-induced phosphorylation of ErbB3 in PAE cells expressing ErbB3 only. Furthermore, it was suggested that ErbB3 was unable to phosphorylate exogenous substrates (13). This could potentially explain HRG-β1-induced inhibition of EGFR downregulation if phosphorylation of adaptor/effector proteins involved in endocytosis was reduced. Additionally, we observed a constitutive basal ErbB3 phosphorylation in cells expressing ErbB3 only. This is in line with data suggesting that overexpression of ErbB3 alone results in weak ErbB3 phosphorylation (12,53). The low constitutive phosphorylation of ErbB3 can possibly be explained by the recent finding that the carboxyl tail of ErbB3, in contrast to the tail of EGFR, cannot interface with the kinase domain and thus lacks autoinhibitory activity (12). The finding that HRG-β1-induced ErbB3 phosphorylation in PAE.ErbB3 cells was blocked by the kinase inhibitor AG1478 supports the notion that ErbB3 has some constitutive kinase activity, even though AG1478 has until now been thought of as EGFR specific. The constitutive as well as the HRG-β1-induced and c-Met-independent ErbB3 phosphorylation in PAE.ErbB3 cells could further suggest that contrary to previously reported results (14), ErbB3 may form active homodimers.

In summary, our results show that ErbB3 is endocytosed in a clathrin-dependent manner in the absence of added ligand and independent of its phosphorylation. Additionally, we observed that while ErbB3 is internalized independently of other ErbB proteins, its dimerization with EGFR negatively impacted on internalization of EGF and downregulation of EGFR from the plasma membrane. This could cause sustained EGF-induced signaling and contribute to the oncogenicity of ErbB3.

Supplementary material

Supplementary Figures S1–S6 can be found at http://carcin.oxfordjournals.org/.

Funding

The Research Council of Norway; The Norwegian Cancer Society; The South-Eastern Norway Regional Health Authority; Torsteds Legacy; Bruuns Legacy; The Jahre Foundation.

Acknowledgements

We are grateful to Marianne Skeie Rødland for valuable technical assistance. PAE cells were a gift from Carl-Henrik Heldin, Uppsala, Sweden, and stably transfected PAE cells expressing the EGFR were given to us by Alexander Sorkin, University of Pittsburgh, USA.

Conflict of Interest Statement: None declared.

References

1. Sweeney,C. *et al*. (2006) ErbB receptor negative regulatory mechanisms: implications in cancer. *J. Mammary Gland Biol. Neoplasia*, **11**, 89–99.
2. Zahnow,C.A. (2006) ErbB receptors and their ligands in the breast. *Expert Rev. Mol. Med.*, **8**, 1–21.
3. Zandi,R. *et al*. (2007) Mechanisms for oncogenic activation of the epidermal growth factor receptor. *Cell. Signal.*, **19**, 2013–2023.
4. Olayioye,M.A. *et al*. (2000) The ErbB signaling network: receptor heterodimerization in development and cancer. *EMBO J.*, **19**, 3159–3167.
5. Ferguson,K.M. *et al*. (2003) EGF activates its receptor by removing interactions that autoinhibit ectodomain dimerization. *Mol. Cell*, **11**, 507–517.
6. Klapper,L.N. *et al*. (1999) The ErbB-2/HER2 oncoprotein of human carcinomas may function solely as a shared coreceptor for multiple stroma-derived growth factors. *Proc. Natl Acad. Sci. USA*, **96**, 4995–5000.
7. Lemmon,M.A. (2009) Ligand-induced ErbB receptor dimerization. *Exp. Cell Res.*, **315**, 638–648.
8. Garrett,T.P. *et al*. (2003) The crystal structure of a truncated ErbB2 ectodomain reveals an active conformation, poised to interact with other ErbB receptors. *Mol. Cell*, **11**, 495–505.
9. Sierke,S.L. *et al*. (1997) Biochemical characterization of the protein tyrosine kinase homology domain of the ErbB3 (HER3) receptor protein. *Biochem. J.*, **322**, 757–763.
10. Guy,P.M. *et al*. (1994) Insect cell-expressed p180erbB3 possesses an impaired tyrosine kinase activity. *Proc. Natl Acad. Sci. USA*, **91**, 8132–8136.
11. Jura,N. *et al*. (2009) Structural analysis of the catalytically inactive kinase domain of the human EGF receptor 3. *Proc. Natl Acad. Sci. USA*, **106**, 21608–21613.
12. Bublil,E.M. *et al*. (2010) Kinase-mediated quasi-dimers of EGFR. *FASEB J.*, **24**, 4744–4755.
13. Shi,F. *et al*. (2010) ErbB3/HER3 intracellular domain is competent to bind ATP and catalyze autophosphorylation. *Proc. Natl Acad. Sci. USA.*, **107**, 7692–7697.
14. Berger,M.B. *et al*. (2004) ErbB3/HER3 does not homodimerize upon neuregulin binding at the cell surface. *FEBS Lett.*, **569**, 332–336.
15. Citri,A. *et al*. (2003) The deaf and the dumb: the biology of ErbB-2 and ErbB-3. *Exp. Cell Res.*, **284**, 54–65.
16. Liles,J.S. *et al*. (2010) ErbB3 expression promotes tumorigenesis in pancreatic adenocarcinoma. *Cancer Biol. Ther.*, **10**, 555–563.
17. Kim,H.H. *et al*. (1994) Epidermal growth factor-dependent association of phosphatidylinositol 3-kinase with the erbB3 gene product. *J. Biol. Chem.*, **269**, 24747–24755.
18. Fedi,P. *et al*. (1994) Efficient coupling with phosphatidylinositol 3-kinase, but not phospholipase C gamma or GTPase-activating protein, distinguishes ErbB-3 signaling from that of other ErbB/EGFR family members. *Mol. Cell. Biol.*, **14**, 492–500.
19. Hellyer,N.J. *et al*. (1998) ErbB3 (HER3) interaction with the p85 regulatory subunit of phosphoinositide 3-kinase. *Biochem. J.*, **333**, 757–763.
20. Hamburger,A.W. (2008) The role of ErbB3 and its binding partners in breast cancer progression and resistance to hormone and tyrosine kinase directed therapies. *J. Mammary Gland Biol. Neoplasia*, **13**, 225–233.
21. Baselga,J. *et al*. (2009) Novel anticancer targets: revisiting ERBB2 and discovering ERBB3. *Nat. Rev. Cancer*, **9**, 463–475.
22. Campbell,M.R. *et al*. (2010) HER3 comes of age: new insights into its functions and role in signaling, tumor biology, and cancer therapy. *Clin. Cancer Res.*, **16**, 1373–1383.
23. Teis,D. *et al*. (2003) The odd couple: signal transduction and endocytosis. *Cell. Mol. Life Sci.*, **60**, 2020–2033.
24. Sorkin,A. *et al*. (2008) Endocytosis and intracellular trafficking of ErbBs. *Exp. Cell Res.*, **314**, 3093–3106.
25. Warren,C.M. *et al*. (2006) Signaling through ERBB receptors: multiple layers of diversity and control. *Cell. Signal.*, **18**, 923–933.
26. Baulida,J. *et al*. (1996) All ErbB receptors other than the epidermal growth factor receptor are endocytosis impaired. *J. Biol. Chem.*, **271**, 5251–5257.
27. Waterman,H. *et al*. (1998) Alternative intracellular routing of ErbB receptors may determine signaling potency. *J. Biol. Chem.*, **273**, 13819–13827.
28. Haslekas,C. *et al*. (2005) The inhibitory effect of ErbB2 on epidermal growth factor-induced formation of clathrin-coated pits correlates with retention of epidermal growth factor receptor-ErbB2 oligomeric complexes at the plasma membrane. *Mol. Biol. Cell*, **16**, 5832–5842.
29. Mimnaugh,E.G. *et al*. (1996) Polyubiquitination and proteasomal degradation of the p185c-erbB-2 receptor protein-tyrosine kinase induced by geldanamycin. *J. Biol. Chem.*, **271**, 22796–22801.
30. Hommelgaard,A.M. *et al*. (2004) Association with membrane protrusions makes ErbB2 an internalization-resistant receptor. *Mol. Biol. Cell*, **15**, 1557–1567.
31. Baulida,J. *et al*. (1997) Heregulin degradation in the absence of rapid receptor-mediated internalization. *Exp. Cell Res.*, **232**, 167–172.
32. Warren,C.M. *et al*. (2006) The N-terminal domains of neuregulin 1 confer signal attenuation. *J. Biol. Chem.*, **281**, 27306–27316.
33. Cao,Z. *et al*. (2007) Neuregulin-Induced ErbB3 downregulation is mediated by a, protein stability cascade involving the E3 ubiquitin ligase Nrdp1. *Mol. Cell. Biol.*, **27**, 2180–2188.
34. Qiu,X.B. *et al*. (2002) Nrdp1/FLRF is a ubiquitin ligase promoting ubiquitination and degradation of the epidermal growth factor receptor family member, ErbB3. *Proc. Natl Acad. Sci. USA*, **99**, 14843–14848.
35. Diamonti,A.J. *et al*. (2002) An RBCC protein implicated in maintenance of steady-state neuregulin receptor levels. *Proc. Natl Acad. Sci. USA*, **99**, 2866–2871.
36. Wu,X. *et al*. (2004) Stabilization of the E3 ubiquitin ligase Nrdp1 by the deubiquitinating enzyme USP8. *Mol. Cell. Biol.*, **24**, 7748–7757.
37. Yen,L. *et al*. (2006) Loss of Nrdp1 enhances ErbB2/ErbB3-dependent breast tumor cell growth. *Cancer Res.*, **66**, 11279–11286.
38. Pedersen,N.M. *et al*. (2009) Expression of epidermal growth factor receptor or ErbB3 facilitates geldanamycin-induced down-regulation of ErbB2. *Mol. Cancer Res.*, **7**, 275–284.
39. Johansen,F.E. *et al*. (2001) The J chain is essential for polymeric Ig receptor-mediated epithelial transport of IgA. *J. Immunol.*, **167**, 5185–5192.
40. Huang,F. *et al*. (2004) Analysis of clathrin-mediated endocytosis of epidermal growth factor receptor by RNA interference. *J. Biol. Chem.*, **279**, 16657–16661.
41. Johannessen,L.E. *et al*. (2006) Activation of the epidermal growth factor (EGF) receptor induces formation of EGF receptor- and Grb2-containing clathrin-coated pits. *Mol. Cell. Biol.*, **26**, 389–401.
42. Grovdal,L.M. *et al*. (2004) Direct interaction of Cbl with pTyr 1045 of the EGF receptor (EGFR) is required to sort the EGFR to lysosomes for degradation. *Exp. Cell Res.*, **300**, 388–395.
43. Longva,K.E. *et al*. (2005) Herceptin-induced inhibition of ErbB2 signaling involves reduced phosphorylation of Akt but not endocytic down-regulation of ErbB2. *Int. J. Cancer*, **116**, 359–367.
44. Chen,X. *et al*. (1996) An immunological approach reveals biological differences between the two NDF/heregulin receptors, ErbB-3 and ErbB-4. *J. Biol. Chem.*, **271**, 7620–7629.
45. Engelman,J.A. *et al*. (2007) MET amplification leads to gefitinib resistance in lung cancer by activating ERBB3 signaling. *Science*, **316**, 1039–1043.
46. Bachleitner-Hofmann,T. *et al*. (2008) HER kinase activation confers resistance to MET tyrosine kinase inhibition in MET oncogene-addicted gastric cancer cells. *Mol. Cancer Ther.*, **7**, 3499–3508.

47. Arteaga,C.L. (2007) HER3 and mutant EGFR meet MET. *Nat. Med.*, **13**, 675–677.
48. Maemura,M. *et al*. (2006) Inhibitory effect of c-Met mutants on the formation of branching tubules by a porcine aortic endothelial cell line. *Cancer Sci.*, **97**, 1343–1350.
49. Berthou,S. *et al*. (2004) The Met kinase inhibitor SU11274 exhibits a selective inhibition pattern toward different receptor mutated variants. *Oncogene*, **23**, 5387–5393.
50. Park,Y.J. *et al*. (2010) Macrophage inhibitory cytokine-1 transactivates ErbB family receptors via the activation of Src in SK-BR-3 human breast cancer cells. *BMB Rep.*, **43**, 91–96.
51. Contessa,J.N. *et al*. (2006) Compensatory ErbB3/c-Src signaling enhances carcinoma cell survival to ionizing radiation. *Breast Cancer Res. Treat.*, **95**, 17–27.
52. Ungefroren,H. *et al*. (2011) The Src family kinase inhibitors PP2 and PP1 block TGF-beta1-mediated cellular responses by direct and differential inhibition of type I and type II TGF-beta receptors. *Curr. Cancer Drug Targets.*, **11**, 524–535.
53. Yang,S. *et al*. (2007) Mapping ErbB receptors on breast cancer cell membranes during signal transduction. *J. Cell Sci.*, **120**, 2763–2773.
54. Hanover,J.A. *et al*. (1984) Kinetics of transit of transferrin and epidermal growth factor through clathrin-coated membranes. *Cell*, **39**, 283–293.
55. Motley,A. *et al*. (2003) Clathrin-mediated endocytosis in AP-2-depleted cells. *J. Cell Biol.*, **162**, 909–918.
56. Hughes,J.B. *et al*. (2009) Pertuzumab increases epidermal growth factor receptor down-regulation by counteracting epidermal growth factor receptor-ErbB2 heterodimerization. *Mol. Cancer Ther.*, **8**, 1885–1892.
57. Noguchi,H. *et al*. (1999) Expression of heregulin alpha, erbB2, and erbB3 and their influences on proliferation of gastric epithelial cells. *Gastroenterology*, **117**, 1119–1127.
58. Frolov,A. *et al*. (2007) ErbB3 expression and dimerization with EGFR influence pancreatic cancer cell sensitivity to erlotinib. *Cancer Biol. Ther.*, **6**, 548–554.
59. Yotsumoto,F. *et al*. (2010) Amphiregulin regulates the activation of ERK and Akt through epidermal growth factor receptor and HER3 signals involved in the progression of pancreatic cancer. *Cancer Sci.*, **101**, 2351–2360.
60. Ueno,Y. *et al*. (2008) Heregulin-induced activation of ErbB3 by EGFR tyrosine kinase activity promotes tumor growth and metastasis in melanoma cells. *Int. J. Cancer*, **123**, 340–347.
61. Prigent,S.A. *et al*. (1992) Expression of the c-erbB-3 protein in normal human adult and fetal tissues. *Oncogene*, **7**, 1273–1278.
62. Lemoine,N.R. *et al*. (1992) Expression of the ERBB3 gene product in breast cancer. *Br. J. Cancer*, **66**, 1116–1121.

Received October 17, 2011; revised March 2, 2012; accepted March 14, 2012